Giant Spin Rotation in the Junction between a Normal Metal and a Quantum Spin Hall System

Takehito Yokoyama,[1] Yukio Tanaka,[1] and Naoto Nagaosa[2,3]

[1]*Department of Applied Physics, Nagoya University, Nagoya, 464-8603, Japan*
[2]*Department of Applied Physics, University of Tokyo, Tokyo 113-8656, Japan*
[3]*Cross Correlated Materials Research Group (CMRG), ASI, RIKEN, WAKO 351-0198, Japan*

(Received 30 December 2008; published 21 April 2009)

We study theoretically the reflection problem in the junction between a normal metal and an insulator characterized by a parameter M, which is a usual insulator for $M > 0$ or a quantum-spin-Hall system for $M < 0$. The spin rotation angle α at the reflection is obtained as a function of M and the incident angle θ measured from the normal to the interface. The α shows rich structures around the quantum critical point $M = 0$ and $\theta = 0$; i.e., α can be as large as $\sim\pi$ at an incident angle in the quantum spin Hall case $M < 0$ because the helical edge modes resonantly enhance the spin rotation, which can be used to map the energy dispersion of the helical edge modes. As an experimentally relevant system, we also study the spin rotation effect in quantum-spin-Hall–normal-metal–quantum-spin-Hall trilayer junction.

DOI: 10.1103/PhysRevLett.102.166801 PACS numbers: 73.43.Nq, 72.25.Dc, 85.75.−d

The ultimate goal of spintronics is to manipulate spin without a magnetic field, and the relativistic spin-orbit interaction is the key to realize it. One example is the Datta-Das spin transistor [1] where the spin-orbit interaction modified by the gate voltage controls the rotation of the spin of the carriers. However, usually the strength of the spin-orbit interaction is weak and its influence is small, especially in semiconductors. Nevertheless, its effects are now clearly observed experimentally, e.g., in the Rashba spin splitting [2], and spin Hall effect (SHE) [3–6]. Further enhancement of the spin-orbit effects in semiconductors is highly desired, and for that purpose we propose in this Letter to use the quantum-spin-Hall (QSH) system [7,8] and its junction to the normal metal (N) as the spin rotator with a giant angle α of the order of π due to the resonance with the helical edge channels. This effect can be used to map the energy dispersion of the helical edge modes, and also to produce the spin current parallel to the interface with the average over the incident angle.

Naively, QSH system can be regarded as the two copies of the integer quantum Hall systems for up and down spins with the opposite chiralities. Hence, the chiral edge modes for up and down spins with the opposite propagating directions are expected, which is called the helical edge modes [9–12]. Two sets of the helical edge modes can be mixed by, e.g., the impurity scattering, and open the gap, but when the number of these sets is odd, i.e., $Z_2 = 1$, there always remains a helical mode pair which is protected by the Kramers theorem associated with the time-reversal symmetry. The phase transition between the trivial insulator ($Z_2 = 0$), and the topological insulator ($Z_2 = 1$) occurs at the gap closing point, where the mass of the Dirac Fermion changes sign [13,14].

The existence of the QSH state has been predicted in semiconductors with an inverted electronic gap in HgTe/CdTe quantum wells [13]. The quantum well system experiences a quantum phase transition by changing the thickness. Recent experiments have successfully demonstrated the existence of the helical edge mode for the quantum well of the HgTe system by the measurement of the quantized charge conductance [15]. Also recently, one can obtain the system very close to the quantum critical point by tuning the thickness of the quantum well [16].

Most of the previous works on QSH states have focused on properties of the isolated QSH system, in particular, edge states of the system. However, in experiments to detect some characteristics of the QSH system, some probe, e.g., a (metallic) electrode should be attached to the QSH. Therefore, it is important to clarify transport properties in N/QSH junctions. Moreover, the spin transport related to the QSH system is the most interesting issue, which has not been well explored, and we will address it in this Letter. Especially, we focus on the spin transport properties *normal* to the edge of the sample, while most of the previous works are interested in the charge transport *along* the edge channel.

In this Letter, we study a reflection of the electronic wave at the N/QSH interface. It is found that an electron injected from the normal metal shows a spin-dependent reflection at the interface leading to the spin rotation. The spin rotation angle α shows rich structure centered around the quantum critical point $M = 0$, and the normal incident angle $\theta = 0$; i.e., it has a large value comparable to π and even a winding by 4π in the (θ-M)-plane in the QSH region ($M < 0$), which stems from the helical edge modes. This is in sharp contrast to the case of normal-metal–usual-insulator interface ($M > 0$), where the spin rotation angle α does not show peak structures and is much smaller than that in $M < 0$. As an experimentally relevant system, we also investigate multiple reflections in the

QSH/N/QSH junction. It is clarified that the multiple reflection strongly enhances the spin rotation.

Let us commence with the effective four-band model proposed for HgTe/CdTe quantum wells [17]

$$\mathcal{H} = \begin{pmatrix} h(k) & 0 \\ 0 & h^*(-k) \end{pmatrix}, \tag{1}$$

with $h(k) = \epsilon(k) I_{2\times 2} + d_a(k)\sigma^a$, $\epsilon(k) = C - D(k_x^2 + k_y^2)$, $d_a(k) = (Ak_x, -Ak_y, M(k))$, and $M(k) = M - B(k_x^2 + k_y^2)$, where we have used the basis order $(|E_1+\rangle, |H_1+\rangle, |E_1-\rangle, |H_1-\rangle)$ ("E" and "H" represent the electron and hole bands, respectively), and, A, B, C, D, and M are material parameters that depend on the quantum well geometry. $\epsilon(k)$ is the averaged energy dispersion, while $M(k)$ is the their difference between the valence and conduction bands. A represents the strength of the band mixing due to the spin-orbit interaction. $\mathcal{H}$ is equivalent to two copies of the massive Dirac Hamiltonian but with a k-dependent mass $M(k)$ [17]. This model is derived from the Kane model near the Γ point in a quantum well of the HgTe/CdTe junction based on the symmetry arguments of the bands, and its validity is limited only near the Γ point, namely, for small values of k_x and k_y. In this system, the transition of electronic band structure occurs from a normal to an inverted type when the thickness of the quantum well is varied through a critical thickness. This corresponds to the sign change of the mass M of this system [13,18]. It should be noted that since $h(k) \neq h^*(-k)$ (which corresponds to the fact that chirality is different for different spins), spin-orbit coupling has a z component, which leads to the spin rotation effect.

We consider the interface between normal metal and an insulator, the latter of which is an usual insulator for $M > 0$ and a QSH system for $M < 0$, as shown in Fig. 1. For $M < 0$, helical edge modes are expected to appear at the interface [13,18]. The interface is parallel to the y axis and located at $x = 0$, and the energy dispersion of each side is shown schematically in Fig. 1. The insulating side is described by the Hamiltonian given in Eq. (1). The Hamiltonian in the N side is given by setting $A = B = M = 0$ in that of the QSH. The gap $|M|$ opens on the insulating side. $|C|$ is the Fermi energy measured from the bottom of the metallic band. The typical value of $|C|$ in metals is ~ 1 eV.

Now, let us focus on the spin-up state, corresponding to the upper block of the Hamiltonian. The wave function in the N side for the E_1 state injection is given by

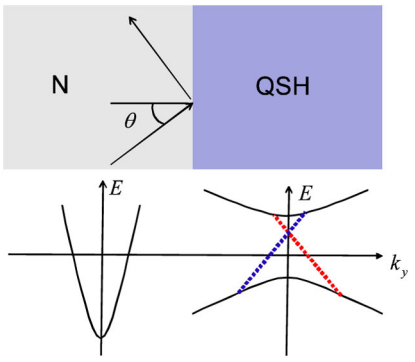

FIG. 1 (color online). N/QSH junction and corresponding band structures (below). Dotted lines represent helical edge modes.

$$\psi(x \le 0) = \left[\begin{pmatrix} 1 \\ 0 \end{pmatrix} e^{ik_F \cos\theta x} + r_E \begin{pmatrix} 1 \\ 0 \end{pmatrix} e^{-ik_F \cos\theta x} + r'_E \begin{pmatrix} 0 \\ 1 \end{pmatrix} e^{-ik_F \cos\theta x} \right] e^{ik_F \sin\theta y} \tag{2}$$

with $k_F^2 = C/D$ and the incident angle θ.

The wave function in the QSH side reads

$$\psi(x \ge 0) = \left[t \begin{pmatrix} Ak_+ e^{i\theta_+} \\ d(k_+) - M(k_+) \end{pmatrix} e^{ik_+ \cos\theta_+ x} + t' \times \begin{pmatrix} Ak_- e^{i\theta_-} \\ d(k_-) - M(k_-) \end{pmatrix} e^{ik_- \cos\theta_- x} \right] e^{ik_F \sin\theta y} \tag{3}$$

with $d(k) = \sqrt{A^2 k^2 + M(k)^2}$ and

$$k_\pm^2 = \frac{1}{2(B^2 - D^2)} \left[-(A^2 - 2MB + 2CD) \pm \sqrt{(A^2 - 2MB + 2CD)^2 - 4(B^2 - D^2)(M^2 - C^2)} \right], \tag{4}$$

which is obtained by solving $E = C - Dk^2 + d(k) = 0$ for k. Here, $\theta_\pm$ denote the incident angles for wave functions with wave number $k_\pm$. In the following, we set $C = 0$ in the insulating side, when the Fermi energy is located at the middle of the gap. Notice that we assume the insulating state so that $k_\pm^2 < 0$. Because of the translational symmetry along the y axis, we have $k_F \sin\theta = k_+ \sin\theta_+ = k_- \sin\theta_-$.

Boundary conditions read $\psi(+0) = \psi(-0)$ and $v_x \psi(+0) = v_x \psi(-0)$ with $v_x = \frac{\partial H}{\partial k_x}$. With these boundary conditions, we can obtain scattering coefficients.

Thus, the reflection coefficients for E_1 state injection are obtained as follows

$$\begin{pmatrix} r_E \\ r'_E \end{pmatrix} = \frac{1}{\Delta_E} \begin{pmatrix} (Ak_+ e^{i\theta_+} - a_+)(d(k_-) - M(k_-) + b_-) - (Ak_- e^{i\theta_-} - a_-)(d(k_+) - M(k_+) + b_+) \\ 2\{-b_+(d(k_-) - M(k_-)) + b_-(d(k_+) - M(k_+))\} \end{pmatrix} \tag{5}$$

with $\Delta_E = (Ak_+ e^{i\theta_+} + a_+)(d(k_-) - M(k_-) + b_-) - (Ak_- e^{i\theta_-} + a_-)(d(k_+) - M(k_+) + b_+)$, $a_\sigma = (1 + \frac{B}{D}) A\lambda_\sigma k_\sigma e^{i\theta_\sigma} - A(d(k_\sigma) - M(k_\sigma))/(2Dk_F \cos\theta)$, $b_\sigma = -A^2 k_\sigma e^{i\theta_\sigma}/(2Dk_F \cos\theta) + (1 - \frac{B}{D})\lambda_\sigma (d(k_\sigma) - M(k_\sigma))$, $\lambda_\sigma = k_\sigma \cos\theta_\sigma/(k_F \cos\theta)$, and $\sigma = \pm$.

The corresponding reflection coefficients for the spin-down state can be obtained by the substitution $A \rightarrow -A$ and $\theta \rightarrow -\theta$. Spin rotation angle α is defined as $\alpha = \mathrm{Im}\log(r_{E\uparrow}/r_{E\downarrow})$, which is the phase difference in the reflection coefficients between up- and down-spin electrons in the E state. From the definition, we see that α is an odd function of θ since $r_{E\uparrow}(-\theta) = r_{E\downarrow}(\theta)$. Note that when the spin of the incident electron is within the xy plane, this angle α gives the spin rotation angle within this plane at the reflection in the same band. Therefore, we call it "spin rotation angle."

Now, we show the results for α in the plane of (θ, M) in Fig. 2 for $C = -0.08$ eV in (a), $C = -0.1$ eV in (b), and $C = -1$ eV in (c) with the other parameters fixed as $A = 4$ eV $\cdot$ Å, $B = -70$ eV $\cdot$ Å^2 and $D = -50$ eV $\cdot$ Å^2. These parameters are appropriate for the HgTe/CdTe quantum well [17]. In Figure 2(a), a sharp ridge in $M < 0$ and $\theta > 0$ region and its negative correspondence in $M < 0$ and $\theta < 0$ are seen. This is in sharp contrast to the usual-insulator case $M > 0$ although α is still nonzero there. Note that the height of the ridge is as high as $\sim\pi/2$. With increasing $|C|$, we find a qualitatively different structure. Near the origin in Fig. 2(b), α reaches π, changes its sign, and *winds by* 4π *around the origin*, while it does not in the region far away from the origin. One might wonder that the singularity occurs at the origin and there is also an endpoint of the "branch cut" separating the 4π winding and no winding. (Note that $\alpha = \pi$ and $\alpha = -\pi$ are equivalent and the continuous increase of α in the clockwise direction is separated into several sheets). In fact, we have checked that $\sin\alpha$, which is physically observable, depends on the direction from which the origin is approached but it does not show any singularity at the endpoint of the "branch cut". As we further increase $|C|$, the branch cuts extend toward the larger $|M|$ and $|\theta|$ region, and approaches gradually to the negative M-axis as shown in Fig. 2(c). Here, one may think that when magnetic field is applied in the xy plane and opens a gap, it will change our results when the Fermi level is inside the gap. However, magnitude of the gap is typically smaller than that of M ($\sim$10 meV), and the Fermi energy is shifted from the crossing of the helical edge dispersions. Hence, our results would be practically robust against applied magnetic field in realistic systems. Note that all these interesting structures occur in the QSH region ($M < 0$). It should be also noticed that these structures are seen for small θ's, i.e., almost normal incidence, and the relevance to the helical edge channel is expected. The angle at which the dispersions of the helical edge modes hit the Fermi energy is given by $\theta_C = \pm\sin^{-1}[\frac{MD}{Ak_F\sqrt{B^2 - D^2}}]$ [18]. We find that a large magnitude of α in Fig. 2 appears around this angle, which means that the helical edge modes resonantly enhance the spin rotation. This is plausible since in the helical edge modes, up and down spins propagate in an opposite direction and hence SU(2) symmetry in spin space is strongly broken there. This is also similar to the Andreev reflection in the superconducting analogue of QSH system where the helical edge channel produces a largely spin-polarized supercurrent at the Andreev reflection [19].

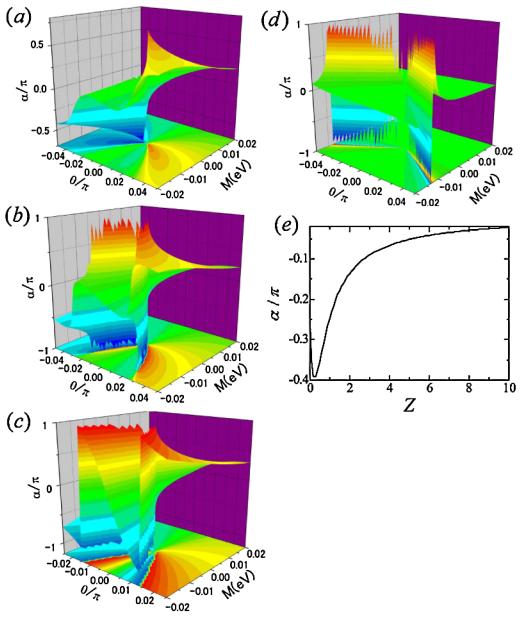

FIG. 2 (color online). Spin rotation angle α as a function of injection angle and M. (a) $C = -0.08$ eV, (b) $C = -0.1$ eV, and (c) $C = -1$ eV. Note that $\alpha = \pi$ and $\alpha = -\pi$ are equivalent and the continuous increase of α in the clockwise direction is separated into several sheets in (b) and (c). Note that $\alpha(-\theta) = -\alpha(\theta)$ is satisfied. Finite barrier potential at the interface is taken into account in (d) and (e). (d) $C = -0.1$ eV and $Z = 10$. (e) α as a function of Z at $M = -0.01$ eV and $\theta = 0.01\pi$.

Now, let us consider the barrier potential at the interface. Considering the Ohmic contact [20], we model the barrier potential at the interface as $U(x) = U\delta(x)$ and introduce dimensionless barrier parameter $Z = U/Dk_F$. We show the result at $Z = 10$ and $C = -0.1$ eV in Fig. 2(d) and also the value at $(M, \theta) = (-0.01$ eV$, 0.01\pi)$ as a function of Z in its realistic region in Fig. 2(e). The peak height away from the helical edge modes is suppressed because the electrons at metallic side "touch" the QSH region less and less as Z increases, while the resonance peak width becomes more and more sharp. This means that the helical edge mode becomes more important. Therefore, the presence of the barrier at the interface does not change our conclusion.

To realize the giant spin rotation experimentally, we propose QSH/N/QSH junction (see the inset in Fig. 3). When N layer is sufficiently thin, the electrons in the N region are in close contact to the QSH systems and the transport property in this junction is determined by the reflection at the interfaces. We will also take statistical and incident angular average of the results in order to obtain more experimentally accessible quantity.

To investigate the spin rotation effect in this junction, we also have to calculate reflection coefficients with the H state injection and E or H state reflection in a similar way.

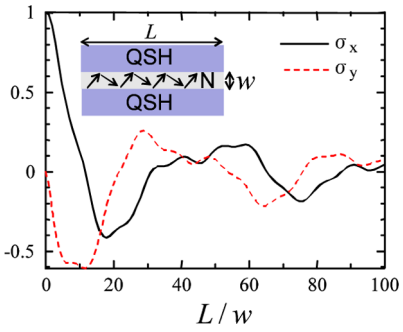

FIG. 3 (color online). Expectation values of σ_x and σ_y as a function of L/w for $C = -1$ eV and $M = -0.01$ eV. Inset shows the model.

We consider the initial wave functions with density matrix as

$$\psi_i = \begin{pmatrix} a_1 \\ a_2 \\ a_3 \\ a_4 \end{pmatrix}, \qquad \overline{a_i^* a_j} = \begin{cases} 1/4 & \text{for } \{i,j\} = \{1,3\},\{2,4\} \\ 0 & \text{otherwise} \end{cases}, \tag{6}$$

where $\overline{\cdots}$ denotes statistical average. The density matrix is chosen so that the initial wave functions have a correlation in the same bands. As seen in Eq. (6), here we consider the initial wave functions with spin polarization along the x axis. Using these expressions, we can obtain expectation values of σ_x and σ_y, Pauli matrices in spin space.

Figure 3 displays expectation values of σ_x and σ_y as a function of L/w for $C = -1$ eV and $M = -0.01$ eV. Here, L and w are the length and width of the N, respectively. An oscillatory dependence on L/w is seen because the phase difference between up- and down-spin states increases with L/w, namely, the number of reflections. When σ_x has an extremum, σ_y almost vanishes and vice versa, which indicates a rotation of the spin in the xy plane in spin space upon propagation in the N of the QSH/N/QSH junction. This means that the predicted giant spin rotation persists and is observable in realistic systems. Around $L/w = 20$, the initial spin is rotated by π. With $w = 5$ nm, this giant spin rotation can be realized with the very short length scale of $L = 100$ nm, which should be compared with that in the previous work [1], where the propagation of electron over 1 μm is required to rotate the electron spin by π. This may be a great advantage for application to nanotechnology.

In summary, we studied a reflection problem at the N/QSH interface and showed that an electron injected from the normal metal in N/QSH junctions shows a spin dependent reflection at the interface and hence there appears a phase difference between up- and down-spin states in the reflection coefficients. The spin rotation angle can be as large as $\sim\pi$ in the QSH junction, because the helical edge modes resonantly enhance the spin rotation. In the QSH/N/QSH junction, multiple reflections at the interfaces increase the phase difference. This also results in a remarkable spin rotation effect in this junction even when the results are averaged over incident angles. The proposed Fabry-Pérot-like heterostructure is experimentally accessible and could be used to unveil another aspect of the QSH state: the *spin rotation effect*.

This work is supported by Grant-in-Aid for Scientific Research (Grants No. 17071007, 17071005, 19048015, and 19048008) from the Ministry of Education, Culture, Sports, Science and Technology of Japan and NTT basic research laboratories. T. Y. acknowledges support by JSPS.

[1] S. Datta and B. Das, Appl. Phys. Lett. **56**, 665 (1990).
[2] J. Nitta, T. Akazaki, H. Takayanagi, and T. Enoki, Phys. Rev. Lett. **78**, 1335 (1997).
[3] M. I. D'yakonov and V. I. Perel', Phys. Lett. A **35**, 459 (1971); JETP Lett. **13**, 467 (1971).
[4] S. Murakami, N. Nagaosa, and S.-C. Zhang, Science **301**, 1348 (2003).
[5] Y. K. Kato, R. C. Myers, A. C. Gossard, and D. D. Awschalom, Science **306**, 1910 (2004).
[6] J. Wunderlich, B. Kaestner, J. Sinova, and T. Jungwirth, Phys. Rev. Lett. **94**, 047204 (2005).
[7] C. L. Kane and E. J. Mele, Phys. Rev. Lett. **95**, 146802 (2005); Phys. Rev. Lett. **95**, 226801 (2005).
[8] B. A. Bernevig and S. C. Zhang, Phys. Rev. Lett. **96**, 106802 (2006).
[9] C. Wu, B. A. Bernevig, and S. C. Zhang, Phys. Rev. Lett. **96**, 106401 (2006).
[10] C. Xu and J. E. Moore, Phys. Rev. B **73**, 045322 (2006).
[11] L. Fu and C. L. Kane, Phys. Rev. B **74**, 195312 (2006); L. Fu and C. L. Kane, Phys. Rev. B **76**, 045302 (2007).
[12] X.-L. Qi, T. Hughes, and S.-C. Zhang, Phys. Rev. B **78**, 195424 (2008).
[13] B. A. Bernevig, T. L. Hughes, and S. C. Zhang, Science **314**, 1757 (2006).
[14] S. Murakami, S. Iso, Y. Avishai, M. Onoda, and N. Nagaosa, Phys. Rev. B **76**, 205304 (2007).
[15] M. König, S. Wiedmann, C. Brüne, A. Roth, H. Buhmann, L. Molenkamp, X.-L. Qi, and S.-C. Zhang, Science **318**, 766 (2007).
[16] L. Molenkamp (private communications).
[17] M. König, H. Buhmann, L. Molenkamp, T. Hughes, C-X Liu, X.-L. Qi, and S.-C. Zhang, J. Phys. Soc. Jpn. **77**, 031007 (2008).
[18] Bin Zhou, Hai-Zhou Lu, Rui-Lin Chu, Shun-Qing Shen, and Qian Niu, Phys. Rev. Lett. **101**, 246807 (2008).
[19] Y. Tanaka, T. Yokoyama, A. V. Balatsky, and N. Nagaosa, Phys. Rev. B **79**, 060505(R) (2009).
[20] Note that if we use a metal such as Au as an N, then the Schottky barrier will not be created [15].